CALCULATION OF INTEGRAL PARAMETERS OF A COMPRESSIBLE TURBULENT BOUNDARY LAYER USING A CONCEPT OF MASS ENTRAINMENT

by

N.M. Standen, B.A.Sc.

A thesis submitted to the Faculty of
Graduate Studies and Research
in partial fulfilment of the requirements
for the degree of Master of Engineering

Department of Mechanical Engineering
McGill University
Montreal

August, 1964

ACKNOWLEDGEMENTS

The author wishes to express his thanks to Professor S. Molder and Dr. B.G. Newman of McGill University, Department of Mechanical Engineering, for their advice and assistance in the analysis of the problem. The guidance of Professor Molder, Director of Research, and his comments during the preparation of this paper were greatly appreciated.

The author is also indebted to Mr. M. Merilo for the preparation of the accompanying figures.

The financial assistance of the Defence Research Board of Canada is gratefully acknowledged.

TABLE OF CONTENTS

LIST OF FIGURES

LIST OF SYMBOLS

$a, b, c,$	Constant Coefficients
a_e, a_o	Sound speed at temperatures T_e and T_o respectively
C_f	Local Skin Friction Coefficient
F	Non-dimensional Mass Entrainment Rate, (Ref. 8)
H	Compressible Shape Factor
H_{tr}	Transformed Shape Factor
H_i	Equivalent Incompressible Shape Factor
$H_{\Delta-\Delta^*}$	Shape Factor associated with Entrainment Rate, Ref.(8)
$q = \rho_e u_e^2$	
M_e	Mach Number at outer edge of Boundary Layer
T	Static Temperature at Height y in Boundary Layer
T_s	Total Temperature at Height y in Boundary Layer
T_e	Static Temperature at outer edge of Boundary Layer
T_o	Total Temperature of external flow
T_{aw}	Adiabatic Wall Temperature
T_w	Wall Temperature
T_r	Reference Temperature
u	Compressible Longitudinal Velocity
U	Transformed Longitudinal Velocity
x	Longitudinal Coordinate Parallel to Wall

X	Transformed Longitudinal Coordinate
y	Coordinate Normal to Wall
Y	Transformed Normal Coordinate
γ	Specific Heat Ratio
δ	Boundary Layer Thickness
δ^*	Compressible Displacement Thickness
δ^*_{tr}	Transformed Displacement Thickness
$\delta^*_i = \Delta^*$	Incompressible Displacement Thickness
θ	Compressible Momentum Thickness
θ_i	Transformed or Incompressible Momentum Thickness
μ	Absolute Viscosity
ρ	Density
Δ	Transformed Boundary Layer Thickness

Subscripts

e	Outer edge of Boundary Layer
o	Evaluated at Total Temperature
r	Evaluated at Reference Temperature
i	Incompressible

SUMMARY

The problem of determining the growth of a turbulent boundary layer under conditions occurring on ramjet air-intakes is discussed. A modified Stewartson transformation is employed to transform the compressible integral momentum equation to an equivalent incompressible plane, adopting approximate temperature-velocity relations of the Crocco and van Driest form. A semi-empirical auxiliary equation, developed by M.R. Head for incompressible flow and using the concept of mass entrainment into the boundary layer, is rearranged for use in the transformed plane. The theoretical results obtained by this method are then compared to McLafferty's lag-length theory, and to experimental data obtained by C.E. Kepler and R.L. O'Brien. It is seen that the mass entrainment theory is in good qualitative agreement with the reported data, and in reasonable quantitative agreement. The latter may be improved by postulating a relationship between temperature and velocity in the boundary layer which is in closer agreement with experiment. It appears that the mass entrainment theory indicates the point of separation of the compressible, turbulent boundary layer, in accordance with conventional incompressible separation criteria.

INTRODUCTION

The study of turbulent boundary layers is generally recognized to be a task of more than slight complexity, for the random eddying motion of the turbulent fluid is not amenable to simple mathematical description. In addition, such phenomena as shearing stresses and heat transfer across a turbulent layer are no longer proportional to parameters which are properties of the fluid alone, as in the case of laminar flows.

The shear stress distribution is not known analytically for turbulent motion. Therefore, the averaged or integral method is widely used in analyzing turbulent boundary layers, since a knowledge of the shear stress variation is not required in this method. For most engineering applications, the solutions of the integral equations provide sufficient information. The momentum thickness yields a measure of the drag on the surface due to the viscosity of the fluid and the displacement thickness accounts for the modification of the inviscid flow field about the surface again due to the fluid viscosity. The behavior of these parameters in many cases also yields information concerning the separation of the flow from the surface.

Such prediction of separation is primarily based on the magnitude and behavior of the ratio of displacement thickness to momentum thickness (Ref. 1). This ratio, known as the shape factor, is a parameter of the integral momentum equation and must be determined in the course of calculation. This entails the use of an auxiliary equation describing the variation of the shape factor. Such an equation is usually empirical or semi-empirical, since the concepts of conservation of mass, momentum and energy in the boundary layer do not yield a relation involving the shape factor variation.

Several auxiliary equations, used in conjunction with the von Karman (integral) momentum equation, have yielded satisfactory results for incompressible flows (Ref. 1). For compressible flow, however, largely due to the lack of experimental data in the supersonic Mach Number range, few original auxiliary equations have been developed. A notable exception is the lag-length theory of G.H. McLafferty and R.E. Barber (Ref. 2). For the most part, auxiliary equations for compressible turbulent boundary layers have been obtained through the use of a mathematical transformation. Using such a transformation, the compressible integral momentum equation is reduced to the incompressible form and is then used in conjunction

with an auxiliary equation obtained from experiments with incompressible fluids. The transformation thus allows the application of the large amount of incompressible data to compressible flows. It has been demonstrated (Ref. 3 and Ref. 4) that a modified form of the Stewartson-Illingworth transformation may be applied to the compressible turbulent momentum equation, thus reducing it to the incompressible form. Perhaps the best known application of such a method is that of Reshotko and Tucker (Ref. 5).

Methods involving the use of transformations have not met with a great deal of success in the past, largely because of difficulties with the auxiliary equations. In addition, the variation of density across the boundary layer, which must be considered in compressible flows, is difficult to describe analytically. Such a description requires the solution of the energy equation, usually in a form yielding a relation between temperature and velocity in the boundary layer. Under certain conditions, such a solution may be achieved, (Ref. 1) but the simultaneous occurrence of heat transfer to the surface and pressure gradients in the flow direction violate the required conditions. A temperature-velocity relationship including the effects of heat transfer and pressure

gradient is unavailable at this time.

In addition to such phenomena as compressibility of the fluid, adverse pressure gradients in the flow direction and heat transfer between the fluid and its bounding surface, other complexities such as centrifugal forces acting on the fluid (which have been neglected in the order of magnitude analysis of the boundary layer equations) and surface roughness are often engineering realities which cannot be ignored. An example of knowing accurately the behavior of boundary layers under these conditions is found in the study of supersonic combustion ramjets. The inlet diffuser of such a ramjet is a non-adiabatic surface over which flows high Mach Number air under an adverse pressure gradient. Due to the high recovery temperatures of high speed flight, the inlet surface must necessarily be cooled, resulting in heat transfer from the fluid to the surface. These are the basic conditions experienced by a turbulent boundary layer on a ramjet diffuser, and consequently comprise the parameters of this analysis.

ANALYSIS

In the following analysis, an ideal gas has been assumed, with a specific heat ratio of 1.4. The

experiment with which the theoretical results were compared was performed at a total temperature of about 400°F and a maximum Mach Number of 6, (Ref. 6) and it was felt that the ideal gas assumptions were sufficiently accurate in this thermodynamic regime. Real gas effects may be included without too much alteration or difficulty.

(A) Momentum Equation

The integral momentum equation for compressible turbulent flow is obtained by integrating the Prandtl momentum equation across the boundary layer thickness (Ref. 1). If the turbulent flow properties are represented as the sum of time-mean values and fluctuating components, then certain terms involving the fluctuating components appear in the integral momentum equation (Ref. 7). These terms usually may be neglected except in the region of separation or in the presence of large centrifugal forces acting on the fluid (Ref. 6 and 7). In Ref. 6 it is observed that these fluctuation terms, which include the variation of static pressure in the direction normal to a curved compression surface, may be neglected for moderately curved surfaces. Thus, the compressible integral momentum equation becomes

$$\frac{d\theta}{dx} + \frac{\theta}{M_e}\frac{dM_e}{dx}\left(\frac{2 + H - M_e^2}{T_o/T_e}\right) = \frac{C_f}{2} \qquad (2)$$

Normal pressure gradients due to centrifugal forces may be neglected on compression surfaces where the radii of curvature are large in comparison with the boundary layer thickness.

The skin friction coefficient C_f must also be defined for turbulent flow. In the present analysis, the Ludwig-Tillman equation for incompressible flow is used, with fluid properties evaluated at Eckert's reference temperature, following the procedure of Ref. 5. The resulting expression employing Sutherland's law of viscosity is

$$\frac{C_f}{2} = \left[.123\ \exp(-1.56H_i)(U_e\theta_i\rho_o/\mu_o)^{-.268}\right]\times$$

$$\times\left[\frac{T_e}{T_r}\left(\frac{T_r}{T_o}\right)^{.402}\left(\frac{T_o + 198}{T_r + 198}\right)^{.268}\right] \qquad (3)$$

The momentum equation is now transformed to a form similar to the integral momentum equation for incompressible flow. A modified Stewartson transformation (Ref. 3 and 4) is used. Defining the transformation for the normal coordinate by

$$dY = \frac{\rho a_e}{\rho_o a_o} dy \tag{4}$$

and equating the compressible stream function to the transformed stream function, there results

$$U = \frac{a_o}{a_e} u \tag{5}$$

Under the transformation, the velocity ratio u/u_e is equal to the ratio of transformed velocities U/U_e.

Employing the Stewartson transformation to the integral boundary layer quantities, then, and recalling that the static pressure remains constant through the boundary layer, the transformed integral parameters are defined (Ref. 4) as

$$\theta_i = \left(\frac{T_e}{T_o}\right)^3 \theta \tag{6}$$

$$\delta^*_{tr} = \int_o^{\Delta} \left(\frac{T_s}{T_o} - \frac{U}{U_e}\right) dY \qquad \text{(See App. A)}$$

$$H_{tr} = \frac{\delta^*_{tr}}{\theta_i} \quad ; \quad H = \frac{T_o}{T_e} H_{tr} + \frac{T_o}{T_e} - 1$$

Substituting equations (6) into the

compressible momentum equation (2), the transformed momentum equation is obtained

$$\frac{d\theta_i}{dx} + \frac{\theta_i}{M_e}\frac{dM_e}{dx}(2 + H_{tr}) = \frac{C_f}{2}\left(\frac{T_e}{T_o}\right)^3 \qquad (7)$$

This transformed equation is still not of the form of the incompressible momentum equation, however, since the transformation of the longitudinal coordinate "x" is undefined, and since the friction coefficient term is not equivalent to the incompressible skin friction. In addition, the transformed shape factor must be related to an equivalent incompressible shape factor.

(B) Temperature Distribution

A relationship between temperature and velocity at any point in the boundary layer is now required in order to relate the transformed shape factor to an equivalent incompressible shape factor (Appendix B).

Such a temperature-velocity relationship was obtained by Crocco as an exact solution of the momentum and energy equations under zero pressure gradient, assuming a Prandtl Number of unity. Van Driest also obtained a similar relationship for a non unit Prandtl Number, although he assumed that the thermal boundary

layer was the same thickness as the velocity layer. The first of these analyses resulted in a linear relationship between temperature and velocity, of the form

$$\frac{T_s}{T_o} = a + b\frac{u}{u_e} \tag{8}$$

with "a" and "b" constant.

Van Driest's equation was a quadratic in velocity ratio,

$$\frac{T_s}{T_o} = a + b\frac{u}{u_e} + c\left(\frac{u}{u_e}\right)^2 \tag{9}$$

The second derivative of this relation is positive, after evaluation of the constants from the boundary conditions.

However, under adverse pressure gradients, temperature-velocity curves obtained from experiments (Ref. 6) exhibit a negative second derivative (Fig. 6). It appears that the temperature distribution is at least of second order in velocity ratio, and has coefficients which yield negative second derivatives when the pressure gradient is considered.

The difficulty in obtaining an equation for

the temperature distribution suggests the use of a simpler, although less accurate approximation. Consequently, both the Crocco and Van Driest temperature distributions were used. Since the temperature distribution appears in integral or averaged relations only, the resulting error is not too severe.

(C) Auxiliary Equation

In either the compressible or transformed momentum equations, it is still necessary to evaluate the shape parameter H. Since this shape factor varies with the growth of the boundary layer, an equation defining its variation must be obtained.

A concept of the rate of entrainment of external flow into the incompressible turbulent boundary layer, suggested by M.R. Head (Ref. 8), has led to the formulation of an auxiliary equation describing the shape parameter variation. Head's auxiliary equation is a more promising approach to the problem since it involves the investigation of a physical phenomenon which is the basis of boundary layer growth.

In his derivation, (Ref. 8), Head assumes that the rate of entrainment into a turbulent boundary layer depends upon a boundary layer thickness

parameter, the free stream velocity and the velocity distribution in the outer portion of the layer. Using non-dimensional terms, Head arrived at a form of the auxiliary equation

$$\frac{d}{dX}(\Delta - \Delta^*) = F - (\Delta - \Delta^*)/M_e \frac{dM_e}{dX} \qquad (10)$$

Using the experimental results of several papers, Head obtained an empirical correlation between the function $F(H_{\Delta-\Delta^*})$ and the shape factor $H_{\Delta-\Delta^*} = (\Delta - \Delta^*)/\theta_i$, and a correlation between $H_{\Delta-\Delta^*}$ and H_i, Figs. (1) and (2). It should be emphasized that these results were obtained for incompressible flow.

(D) Solution of the Equations

The transformation of the momentum equation is completed by defining the x-coordinate transformation as

$$\frac{dX}{dx} = \frac{T_e}{T_r}\left(\frac{T_e}{T_o}\right)^3 \left(\frac{\mu_r}{\mu_o}\right)^{.268} \qquad \text{(Ref.(3) and Appendix C)}$$

and by relating the transformed and equivalent incompressible shape factors (Appendix B).

Head's auxiliary equation, Eqn.(10), is put into workable form by fitting equations to the curves

in Figs. (1) and (2). The equations so obtained are

$$H_{\Delta-\Delta^*} = 1.535\ (H_i - .7)^{-2.715} + 3.3 \qquad (11)$$

corresponding to Fig. (2), and

$$F = .0306\ (H_{\Delta-\Delta^*} - 3.0)^{-.653} \qquad (12)$$

corresponding to Fig. (1).

The resulting form of the auxiliary equation is

$$\frac{dH_i}{dx} = -\frac{(H_i-.7)^{3.715}}{4.17}\left[\frac{F}{\theta_i}\frac{dX}{dx} - \frac{H_{\Delta-\Delta^*}}{M_e}\frac{dM_e}{dx} - \frac{H_{\Delta-\Delta^*}}{\theta_i}\frac{d\theta_i}{dx}\right] \qquad (13)$$

where $H_{\Delta-\Delta^*}$ and F are given by Eqn. (11) and (12). The derivation of this form is presented in Appendix C.

The momentum and auxiliary equations were solved using a simultaneous numerical solution of the Runge-Kutta type. The integral parameters so computed were then transformed to the compressible plane by means of Eqn. (6).

COMPARISON WITH EXPERIMENT

A comparison of the calculation results with experiment will be limited to four sets of data obtained by Kepler and O'Brien (Ref. 6). This data consists of boundary layer measurements on flat plates at Mach Numbers of 3 and 6, a circular arc compression surface at an initial Mach Number of 3 and an isentropic compression ramp at Mach 6. Two different rates of wall cooling have been applied to each surface. Although these measurements appear to be quite precise, any conclusions which are drawn on the basis of such a limited comparison must be regarded as preliminary observations.

A. Mach 3 Flat Plate

The cross plot of the velocity and temperature profiles reported by Kepler and O'Brien is shown in Fig.(5). The Crocco temperature-velocity relation appears to be a good approximation to both the cooled and uncooled wall conditions. The quadratic temperature-velocity relationship (Eqn.(9) and Appendix B(b)) would afford a better fit for the uncooled wall case, but at a Mach Number of 3 and at the high wall temperature the difference between the linear and quadratic relations is small. For convenience, therefore, the Crocco relation

was used.

The variation of momentum thickness and displacement thickness with distance along the flat plate is presented in Fig.(6). The theoretical variation is in good qualitative and quantitative agreement with experiment, any discrepancies being within the magnitude of the repeatability of the experiment. The McLafferty lag-length prediction of the uncooled momentum thickness is not shown as it is coincident with the corresponding curve of the mass entrainment theory.

B. Mach 6 Flat Plate

The calculation results for the flat plate at Mach 6, Fig.(8), do not show as good agreement with experiment as in the Mach 3 case. It is difficult to compare the theory with the experiment qualitatively since only three measurements of the boundary layer parameters were made. However, it is seen from experiment that the momentum thickness of the boundary layer over the cooled wall is greater than the momentum thickness of the flow over the uncooled wall. It appears that the magnitudes of these thicknesses become nearly equal in the downstream direction but such a trend cannot be established due both to the lack of further experimental points and to the experimental error involved,

represented by the repeatability of the measurement. The mass entrainment theory indicates that the cooled momentum thickness increases at a slower rate than the uncooled thickness, and that the magnitude of the cooled boundary layer momentum thickness eventually becomes less than the magnitude of the uncooled momentum thickness. On the other hand, McLafferty's lag-length theory predicts the same trends exhibited by the experiment. For the uncooled wall case, the mass entrainment theory and the lag-length theory are in close agreement.

Neither the mass entrainment theory nor the lag-length theory yield good quantitative agreement with the experimental variation of displacement thickness, although both exhibit the same qualitative behavior as the experimental data. The magnitude of the cooled displacement thickness as given by the mass entrainment theory could be increased and thus improved by using a temperature-velocity relationship in closer agreement with experiment. The experimental temperature relation is illustrated in Fig.(7).

The temperature-velocity curve obtained from experiment is well approximated, in the uncooled wall case, by the Crocco relation. In the absence of a pressure gradient, the quadratic relation should yield the best description of the actual temperature-velocity

curve, as in Fig.(5a) and (12a). However, a small adverse pressure gradient was reported to exist on the flat plate at Mach 6 and this factor caused the deviation of the temperature-velocity curve from that predicted by the quadratic relation to a form more closely described by the Crocco linear equation. The temperature distribution in the boundary layer over the cooled wall is at variance with even the Crocco relation, suggesting that another factor in addition to the adverse pressure gradient must be considered. This is discussed more fully in a later section.

The existence of the adverse pressure gradient was taken into account in both the momentum and auxiliary equations. Following the argument set forth in the ANALYSIS, the Crocco temperature-velocity relation was not corrected for adverse pressure gradient effects in the cooled wall case.

C. Mach 3 Circular Arc Surface

The Mach Number distribution on the circular arc surface, reported in Ref. 6, was described analytically by a series of linear and semi-logarithmic equations. Each of these equations was chosen to represent best the experimental Mach Number data within a particular interval on the compression surface.

The temperature-velocity relations obtained

from the data of Ref. 6 are illustrated in Fig.(5) and (9). Figure (5) shows the relationship at the beginning of compression, under a negligible pressure gradient. It is identical to the case of the flat plate at Mach 3. Figure (9) depicts the temperature-velocity relationship at the end of compression, where the adverse pressure gradient is present, for both the cooled and uncooled wall conditions. It is seen in Fig. (9) that the experimental points are reasonably well approximated by the Crocco linear relation in the uncooled boundary layer. The temperature relation in the cooled boundary layer, however, is in poor agreement with Crocco's linear relation, and vividly exhibits the negative second derivative characteristic of the temperature-velocity profiles from Ref. 6 under adverse pressure gradients with considerable heat transfer.

The curves of the variation of momentum thickness, Fig. (10), and displacement thickness, Fig. (11), with distance along the circular arc are in poor quantitative agreement with experiment. Qualitatively, however, the mass entrainment theory does bear some resemblance to the experimental variations. In this respect it is more accurate than McLafferty's lag-length theory, also shown in these figures. McLafferty's theory does predict values of the momentum and displacement thicknesses which are nearer in magnitude to the

experimental results than is the mass entrainment theory. This is more or less expected since the lag-length theory was formulated on the basis of experimental results obtained in the Mach 3 range on various compression surfaces, some of which were similar to the circular arc under consideration.

The experimental momentum thickness, Fig.(10), shows a larger value initially for the cooled wall than for the uncooled surface. The cooled momentum thickness remains greater than the uncooled thickness to a distance of approximately 7.6 inches along the surface (1.6 inches downstream of the start of compression). At this point the uncooled momentum thickness, increasing rapidly, exceeds the cooled values. This same trend is predicted by the mass entrainment theory, although the slopes of the theoretical curves for both wall cooling rates are negative at the start of compression, while the slopes of the experimental curves are nearly zero, or slightly positive in the uncooled case.

The same qualitative agreement is apparent concerning the displacement thickness variation, Fig.(11). According to the data of Ref. 6, the magnitude of the uncooled displacement thickness is greater than that of the cooled displacement thickness at all points on the

compression surface. This same behavior is predicted by the mass entrainment theory, which also indicates a more rapidly increasing magnitude of the uncooled displacement thickness in comparison to the cooled displacement thickness. This comparison is also evident in the experimental data. Again, however, the mass entrainment theory predicts decreasing values of both uncooled and cooled displacement thickness after the start of compression, whereas the experimental values in this region show only a small decrease in the cooled boundary layer, and nearly constant values for the uncooled flow.

Improvement in the values of cooled displacement thickness could be achieved if an analytic relation between temperature and velocity, more closely approximating the experimental relation at all points on the compression surface, were used. Mathematically, from Eqn.(A5), it is seen that values of the total temperature ratio Ts/To greater than those predicted by the Crocco relation would yield larger values of the transformed displacement thickness, and thus, in equation (A4), larger values of the compressible displacement thickness. The increase of displacement thickness values would be reflected to a lesser degree in the values of the momentum thickness, which would also tend to

increase. Since the values of both the momentum thickness and displacement thickness at the start of compression ($x = 6.0$ in.) are fixed as initial or starting conditions in the calculation, the increase of the integral parameters at succeeding points on the surface would reduce the negative slopes of the theoretical curves for the cooled boundary layer, and bring the curves into closer agreement with experiment. This improvement is discussed more fully in a later section.

Little improvement in the curves of the uncooled thicknesses could be expected by means of this correction, however, since the Crocco temperature-velocity equation provides good agreement with the experimental relations throughout the compression. Indeed, it is not expected that an adjustment to the cooled temperature relation would induce sufficient improvement in the curves of the cooled thicknesses to provide satisfactory agreement with experiment. Some additional factor must be considered in the flow over this particular compression surface, and this factor should be common to both the uncooled and cooled conditions. It is suggested that the consideration of centrifugal forces in the boundary layer may provide the necessary correction to the curves. An analysis of the magnitude of terms in the integral momentum equation

at the start of compression for the uncooled flow case indicated that a relatively small positive addition to the right side of Eqn. (7) would change the slope of the compressible momentum thickness curve from a negative value to a small positive value. An order of magnitude analysis indicated that the inclusion of centrifugal force effects in the momentum equation would provide at least a partial correction in the desired direction. However, the difficulty of describing these effects analytically in the integral momentum equation precluded their immediate application in the circular arc case. Of the four experimental surfaces considered in this study, it is expected that centrifugal force effects would be of importance only on the circular arc, due to the relatively smaller ratio of the boundary layer thickness to radius of curvature of that surface.

D. Mach 6 Isentropic Surface

An examination of the velocity profiles reported by Kepler and O'Brien, Figs. (3) and (4) indicates a full profile for both the uncooled and cooled surfaces at the initiation of compression, and inflected profiles for both wall temperatures in the final stages of compression.

Using such profiles in conjunction with total

temperature profiles obtained by Kepler and O'Brien at five stations on the compression surface, temperature-velocity curves were plotted. Examples of these are given in Figs. (12) and (13). It was observed that the van Driest temperature-velocity relation provided good agreement with the experimental points over more than half of the compression surface for the uncooled wall condition. In the case of the cooled wall, neither the van Driest nor the Crocco relation lay among the experimental points, but the Crocco distribution was the nearer of the two. Consequently in accordance with the argument set forth in ANALYSIS, the van Driest relation was used for the calculation of the uncooled boundary layer, and the Crocco equation for the cooled layer.

The calculation results are shown in Figs. (14) and (15). These curves indicate a better qualitative than quantitative agreement with experiment, although the uncooled wall results are in reasonable proximity to the experimental points. This is believed to be due to the closer agreement between the van Driest temperature distribution and experiment in the uncooled wall case, than between the Crocco relation and experiment in the cooled boundary layer. As a check on this assumption, the van Driest relation, giving even poorer agreement with experiment than the Crocco equation (Fig.(13)) was

used in the cooled wall calculation. The values of both the momentum thickness and displacement thickness were found to be lower at all points on the compression surface than those obtained using the Crocco relation. Although the difference was not great (of the order of 5%) it was significant enough to indicate that a closer approximation to the true temperature-velocity relationship would yield better values of the integral parameters.

The calculation of the integral parameters using McLafferty's lag-length procedure was performed by Kepler and O'Brien, and is shown in Figs. (14) and (15). It is noted that the results of the lag-length theory indicate no increase in either the momentum thickness or displacement thickness in the final stages of compression, as is shown by the experimental data. The mass-entrainment method, however, does indicate such an increase, or at least a levelling-off, of the integral values in this region. The value of the equivalent incompressible shape factor, H_i, was between 2.4 and 5.0 at this point, and was increasing rapidly. Such behavior of the shape factor in incompressible flow is generally accepted as a criterion of incipient separation. Although Kepler and O'Brien reported no occurrence of separation in their experiment (Ref. (6)),

the existence of inflected profiles and the increase of integral values suggest that separation was approaching. As was pointed out in Ref. (6), the expansion of the flow at the end of the compression surface, occurring when the flow was returned to its original direction, could well have influenced the behavior of the boundary layer in this region. The influence would be exhibited mainly in the subsonic portion of the boundary layer near the wall, and would have the effect of relaxing the inflected velocity profile, thus discouraging separation.

The calculation of the boundary layer presented here is a first order consideration. The addition of the displacement thickness to the surface profile would modify the Mach Number distribution, especially near the end of compression where the displacement thickness increases rapidly. In this region, the modification would result in a locally increased adverse pressure gradient. One would expect that this result, when included in the calculation, would tend to increase the theoretical values of the integral parameters in this area.

E. Modification of Temperature-Velocity Relation

In the preceding discussion, it has been noted that the existence of an adverse pressure gradient causes the experimental temperature-velocity relationship

in the boundary layer to deviate from the flat plate van Driest quadratic relation. It is also noted that this deviation is always in a direction such that the total temperature ratio is greater than the van Driest value at a given value of the velocity ratio. This deviation is expected, since the quadratic temperature-velocity equation (Eqn.(9) and App.B(b)) was derived on the basis of zero pressure gradient. The effect of an adverse pressure gradient is to retard the fluid near the surface and so reduce the fluid velocity across most of the boundary layer (Fig.4), causing only minor changes in the temperature profile (Ref. 6). The modification of the velocity profile under the adverse pressure gradient results in a larger total temperature ratio at a given velocity ratio than for the zero pressure gradient, or flat plate case.

For the near-adiabatic (uncooled) surfaces described in Ref. 6, the linear Crocco equation (Eqn.(8)) provides reasonably satisfactory agreement with the experimental temperature-velocity curves in the presence of adverse pressure gradients (Fig.(9a) and (13a)). It is emphasized that such agreement is not due to the inclusion of pressure gradient effects in the Crocco equation, for this equation was derived also on the basis of zero pressure gradient. The agreement is

due to the approximate linearity of the experimental data points, and thus is largely fortuitous.

The experimental temperature-velocity relations in the boundary layers over the cooled compression surfaces of Ref. 6 are another matter, however. The linear Crocco relation yields either poor agreement or no agreement at all. Since the cooled flow over either of the compression surfaces is under the same external pressure gradient as the uncooled flow (neglecting the modification of the inviscid flow field due to the boundary layer), the temperature-velocity relation for both rates of heat transfer would be expected to show the same deviation from the quadratic equation. Indeed, the process of cooling the boundary layer increases the velocity of the fluid in the layer as compared to the uncooled flow. On the basis of the argument presented above, the increase of velocity should reduce the deviation of the experimental temperature-velocity relation. Such is not the case, however, and the explanation for the reported temperature-velocity relationships is most likely to be found in the method by which the wall was cooled. As described in Ref. 6, the boundary layer developed initially over an uncooled surface upstream of the test surface. At some distance upstream of the model cooling was applied to the

area on which the boundary layer was growing, and was continued to the end of the test surface. Kepler and O'Brien pointed out that under this system only the portion of the boundary layer near the wall would be cooled. The upper regions would have insufficient time to adjust to the heat transfer at the wall surface. Consequently, the major portion of the boundary layer away from the wall would exhibit higher total temperatures than would be found at corresponding levels in a fully cooled boundary layer. In fact, the temperature profiles reported in Ref. 6 indicate total temperatures in the upper two thirds of the cooled boundary layers equal or nearly equal to those in the corresponding uncooled boundary layers. This factor is believed to be principally responsible for the extreme deviations from theory of the cooled temperature-velocity relations.

It is suggested that the reported temperature-velocity curves be approximated by a quadratic relation of the form of Eqn.(9). Such an approximation should not be of a higher degree than a quadratic since the derivation of Appendix B would not then apply.

The coefficient of the second order term (the coefficient "c" in Eqn.(9)) must be negative, in order that the second derivative of the expression be negative and thus describe the correct curvature of the

relationship. The constant term (term "a" in Eqn.(9)) must necessarily equal the ratio of wall temperature to free stream total temperature in order to satisfy the boundary condition at the wall. The remaining coefficient (coefficient "b" in Eqn.(9)) is then defined by the boundary condition at the outer edge of the boundary layer, namely, that the temperature ratio be unity when the velocity ratio is unity. The determination of the value of the coefficient "c" should include consideration of the effects of pressure gradient and heat transfer.

CONCLUSIONS

The conclusions reached in the preceding discussion may be summarized as follows:

(1) The concept of mass entrainment by a turbulent boundary layer appears to provide the basis of a suitable auxiliary equation for calculation of the shape parameter H of the boundary layer. Empirical relations describing such an entrainment in incompressible flow are applicable to compressible flows as well, through a suitably defined mathematical transformation. The good qualitative agreement between experiment and theory obtained through this concept suggests that the entrainment relationship should be investigated further, and established on a better theoretical and mathematical basis.

(2) Better quantitative theoretical results may be expected if a temperature-velocity relationship, providing closer agreement with experiment than the Crocco or van Driest form, is used. This implies the inclusion of pressure gradient and heat transfer effects in such a relationship.

(3) The mass entrainment method indicates separation of the boundary layer in a region where inflected velocity profiles and increasing values of integral parameters were observed in experiment. Separation was indicated by the behavior of the incompressible shape factor H_i, in accordance with the usual criteria for incompressible flow. Further comparison with experiments must be undertaken before the capability of this method to predict incipient separation is established.

REFERENCES

(1) Schlichting, H.; Boundary Layer Theory. McGraw-Hill, New York, 1955.

(2) McLafferty, G.H., Barber, R.E.; Effect of Adverse Pressure Gradients on Characteristics of Turbulent Boundary Layers in Supersonic Streams. Jour. Aero. Sc. vol.29, Jan. 1962.

(3) Culick, F.E.C., Hill, J.A.F.; A Turbulent Analog of the Stewartson-Illingworth Transformation. Jour. Aero. Sc., April, 1958.

(4) Sivells, J.C., Payne, R.G.; A Method of Calculating Turbulent-Boundary-Layer Growth at Hypersonic Mach Numbers. AEDC-TR-59-3, March, 1959.

(5) Reshotko, E., Tucker, M.; Approximate Calculation of the Compressible Turbulent Boundary Layer with Heat Transfer and Arbitrary Pressure Gradient. NACA TN 4154, Dec., 1957.

(6) Kepler, C.E., O'Brien, R.L.; Supersonic Turbulent Boundary Layer Growth over Cooled Walls in Adverse Pressure Gradients. ASD-TDR-62-87, Oct., 1962.

(7) Shapiro, A.H.; The Dynamics and Thermodynamics of Compressible Fluid Flow, Vol.II. Ronald Press Company, New York, 1954.

(8) Head, M.R.; Entrainment in the Turbulent Boundary Layer. ARE R. and M. No. 3125, Sept., 1958.

APPENDIX A

Derivation of Transformed Integral Parameters using Stewartson's Transformation

(a) Momentum Thickness

By definition $$\theta = \int_0^{\delta} \frac{\rho u}{\rho_e u_e} \left(1 - \frac{u}{u_e}\right) dy$$

Substituting equation (4), and recalling that $u/u_e = U/U_e$, we have

$$\theta = \frac{\rho_o a_o}{\rho_e a_e} \int_0^{\Delta} \frac{U}{U_e} \left(1 - \frac{U}{U_e}\right) dY$$

where Δ is the transformed boundary layer thickness. With $\gamma = 1.4$, this becomes

$$\theta = \left(\frac{T_o}{T_e}\right)^3 \theta_i \qquad \text{A 1}$$

where

$$\theta_i = \int_0^{\Delta} \frac{U}{U_e} \left(1 - \frac{U}{U_e}\right) dY \qquad \text{A 2}$$

so $$\theta_i = \theta \left(\frac{T_e}{T_o}\right)^3 \qquad \text{A 3}$$

(b) Displacement Thickness

By definition $$\delta^* = \int_o^{\delta} \left(1 - \frac{u\rho}{\rho_e u_e}\right) dy$$

or $$\delta^* = \int_o^{\delta} \frac{\rho}{\rho_e} \left(\frac{\rho_e}{\rho} - \frac{u}{u_e}\right) dy$$

Again using equation (4), we obtain

$$\delta^* = \frac{\rho_o a_o}{\rho_e a_e} \int_o^{\Delta} \left(\frac{\rho_e}{\rho} - \frac{U}{U_e}\right) dY$$

By assuming constant static pressure normal to the wall,

$$\frac{\rho_e}{\rho} = \frac{T}{T_e}$$

and

$$\delta^* = \left(\frac{T_o}{T_e}\right)^3 \int_o^{\Delta} \left(\frac{T}{T_e} - \frac{U}{U_e}\right) dY$$

now

$$\frac{T}{T_e} = \frac{T_o}{T_e}\left[\frac{T_s}{T_o} - \frac{u_e^2}{2c_p T_o}\left(\frac{u}{u_e}\right)^2\right]$$

$$= \frac{T_o}{T_e}\left[\frac{T_s}{T_o} - \left(1 - \frac{T_e}{T_o}\right)\frac{U}{U_e}^2\right]$$

so $$\frac{T}{T_e} - \frac{U}{U_e} = \frac{T_o}{T_e}\frac{T_s}{T_o} - \left(\frac{T_o}{T_e} - 1\right)\left(\frac{U}{U_e}\right)^2 - \frac{U}{U_e}$$

$$\frac{T}{T_e} - \frac{U}{U_e} = \frac{T_o}{T_e}\frac{T_s}{T_o} - \frac{T_o}{T_e}\frac{U}{U_e} + \frac{T_o}{T_e}\frac{U}{U_e} - \left(\frac{T_o}{T_e} - 1\right)\left(\frac{U}{U_e}\right)^2 - \frac{U}{U_e}$$

Gathering terms

$$\frac{T}{T_e} - \frac{U}{U_e} = \frac{T_o}{T_e}\left(\frac{T_s}{T_o} - \frac{U}{U_e}\right) + \left(\frac{T_o}{T_e} - 1\right)\frac{U}{U_e}\left(1 - \frac{U}{U_e}\right)$$

Then

$$\delta^* = \left(\frac{T_o}{T_e}\right)^3 \int_o^\Delta \left[\frac{T_o}{T_e}\left(\frac{T_s}{T_o} - \frac{U}{U_e}\right) + \left(\frac{T_o}{T_e} - 1\right)\frac{U}{U_e}\left(1 - \frac{U}{U_e}\right)\right] dY$$

or
$$\delta^* = \left(\frac{T_o}{T_e}\right)^3 \left[\frac{T_o}{T_e}\,\delta^*_{tr} + \left(\frac{T_o}{T_e} - 1\right)\theta_i\right] \qquad \text{A 4}$$

using Eqn. (A 2) and defining

$$\delta^*_{tr} = \int_0^\Delta \left(\frac{T_s}{T_o} - \frac{U}{U_e}\right) dY \qquad \text{A 5}$$

Now, using Eqn. (A 4) and (A 1), we obtain

$$H = \frac{\delta^*}{\theta} = \frac{T_o}{T_e} H_{tr} + \frac{T_o}{T_e} - 1 \qquad \text{A 6}$$

where

$$H_{tr} = \frac{\delta^*_{tr}}{\theta_i}$$

APPENDIX B

Derivation of Relations between Shape Factors

(a) Crocco Temperature Distribution

From Eqn. (8) we have

$$\frac{T_s}{T_o} = a + b\,\frac{u}{u_e} = a + b\,\frac{U}{U_e}$$

where, from boundary conditions,

$$a = \frac{T_w}{T_o} \qquad b = 1 - \frac{T_w}{T_o} = 1 - a$$

Then, in Eqn. (A 5),

$$\delta^*_{tr} = \int_0^{\Delta} \left(a + (1-a)\,\frac{U}{U_e} - \frac{U}{U_e} \right) dY$$

$$= \int_0^{\Delta} a\,\left(1 - \frac{U}{U_e}\right)\, dY$$

or

$$\delta^*_{tr} = a\,\delta^*_i = \frac{T_w}{T_o}\,\delta^*_i$$

where

$$\delta^*_i = \int_0^{\Delta} \left(1 - \frac{U}{U_e}\right) dY \quad \text{as usual.}$$

Now, from Eqn. (6)

$$H_{tr} = \frac{\delta^*_{tr}}{\theta_i} = \frac{T_w}{T_o}\,\frac{\delta^*_i}{\theta_i} = \frac{T_w}{T_o}\,H_i \qquad \text{B 1}$$

Then, from Eqn. (A 6)

$$H = \frac{T_w}{T_e} H_i + \frac{T_o}{T_e} - 1 \qquad \text{B 2}$$

(b) van Driest Temperature Distribution

From Eqn. (9) we have

$$\frac{T_s}{T_o} = a + b \frac{u}{u_e} + c \left(\frac{u}{u_e}\right)^2 = a + b \frac{U}{U_e} + c \left(\frac{U}{U_e}\right)^2$$

where the coefficients are defined as

$$a = \frac{T_w}{T_o} \; ; \; b = \frac{T_{aw}}{T_o} - \frac{T_w}{T_o} \; ; \; c = 1 - \frac{T_{aw}}{T_o}$$

and thus $b = \frac{T_{aw}}{T_o} - a = 1 - c - a$

Then, in Eqn. (A 5),

$$\delta^*_{tr} = \int_0^\Delta \left[a + \frac{U}{U_e} (1-c-a) + c \left(\frac{U}{U_e}\right)^2 - \frac{U}{U_e} \right] dY$$

$$= \int_0^\Delta \left[a \left(1 - \frac{U}{U_e}\right) - c \frac{U}{U_e} \left(1 - \frac{U}{U_e}\right) \right] dY$$

so $$\delta^*_{tr} = a \delta^*_i - c \theta_i$$

Then, from Eqn. (6)

$$H_{tr} = a\, H_i - c = \frac{T_w}{T_o} H_i + \frac{T_{aw}}{T_o} - 1 \qquad \text{B 3}$$

And from Eqn. (A 6)

$$H = \frac{T_w}{T_e} H_i + \frac{T_{aw}}{T_e} - 1 \qquad \text{B 4}$$

APPENDIX C

Development of Momentum and Auxiliary Equations

(a) Momentum Equation

From Eqn. (7)

$$\frac{d\theta_i}{dx} + \frac{\theta_i}{M_e}(2 + H_{tr})\frac{dM_e}{dx} = \frac{C_f}{2}\left(\frac{T_e}{T_o}\right)^3$$

or $$\frac{d\theta_i}{dX} + \frac{\theta_i}{M_e}(2 + H_{tr})\frac{dM_e}{dX} = \frac{dx}{dX}\,\frac{C_f}{2}\left(\frac{T_e}{T_o}\right)^3 = \frac{C_f}{2}_i$$

by transforming the longitudinal coordinate "x".

Thus

$$\frac{dX}{dx} = \frac{\frac{C_f}{2}\left(\frac{T_e}{T_o}\right)^3}{\frac{C_f}{2}\,i}$$

where

$$\frac{C_f}{2}\,i = .123\, e^{-1.561\,H_i}\left(\frac{U_e\theta_i\rho_o}{\mu_o}\right)^{-.268}$$

Then, using Eqn. (3),

$$\frac{dX}{dx} = \frac{T_e}{T_r}\left(\frac{T_r}{T_o}\right)^{.402}\left(\frac{T_o + 198}{T_r + 198}\right)^{.268}\left(\frac{T_e}{T_o}\right)^3$$

or $$\frac{dX}{dx} = \frac{T_e}{T_r}\left(\frac{T_e}{T_o}\right)^3\left(\frac{\mu_r}{\mu_o}\right)^{.268} \qquad \text{C 1}$$

(b) Head's Auxiliary Equation

From Eqn. (10)

$$\frac{d}{dX}\ (\Delta-\Delta^*) = F - \frac{(\Delta-\Delta^*)}{M_e}\ \frac{dM_e}{dX}$$

But $$H_{\Delta-\Delta^*} = \frac{\Delta-\Delta^*}{\theta_i}$$

So $$\frac{d}{dX}\ (H_{\Delta-\Delta^*}\ \theta_i) = F - \frac{H_{\Delta-\Delta^*}\ \theta_i}{M_e}\ \frac{dM_e}{dX}$$

or

$$\frac{d}{dx}\ (H_{\Delta-\Delta^*}\ \theta_i) = F\ \frac{dX}{dx} - \frac{\theta_i H_{\Delta-\Delta^*}}{M_e}\ \frac{dM_e}{dx}$$

Then

$$\theta_i\ \frac{dH_{\Delta-\Delta^*}}{dx} = F\ \frac{dX}{dx} - \frac{\theta_i H_{\Delta-\Delta^*}}{M_e}\ \frac{dM_e}{dx} - H_{\Delta-\Delta^*}\ \frac{d\theta_i}{dx}$$

or

$$\frac{dH_{\Delta-\Delta^*}}{dx} = \frac{F}{\theta_i}\ \frac{dX}{dx} - \frac{H_{\Delta-\Delta^*}}{M_e}\ \frac{dM_e}{dx} - \frac{H_{\Delta-\Delta^*}}{\theta_i}\ \frac{d\theta_i}{dx}$$

But

$$\frac{dH_{\Delta-\Delta^*}}{dx} = \frac{\partial H_{\Delta-\Delta^*}}{\partial H_i}\ \frac{dH_i}{dx}$$

and, from Eqn. (11)

$$\frac{\partial H_{\Delta-\Delta^*}}{\partial H_i} = -4.17\ (H_i - .7)^{-3.715}$$

So $$\frac{dH_i}{dx} = -\frac{(H_i - .7)^{3.715}}{4.17}\left[\frac{F}{\theta_i}\frac{dX}{dx} - \frac{H_{\Delta-\Delta^*}}{M_e}\frac{dM_e}{dx} - \frac{H_{\Delta-\Delta^*}}{\theta_i}\frac{d\theta_i}{dx}\right] \qquad C\ 2$$

where $\frac{dX}{dx}$ is given by Eqn. (C 1)

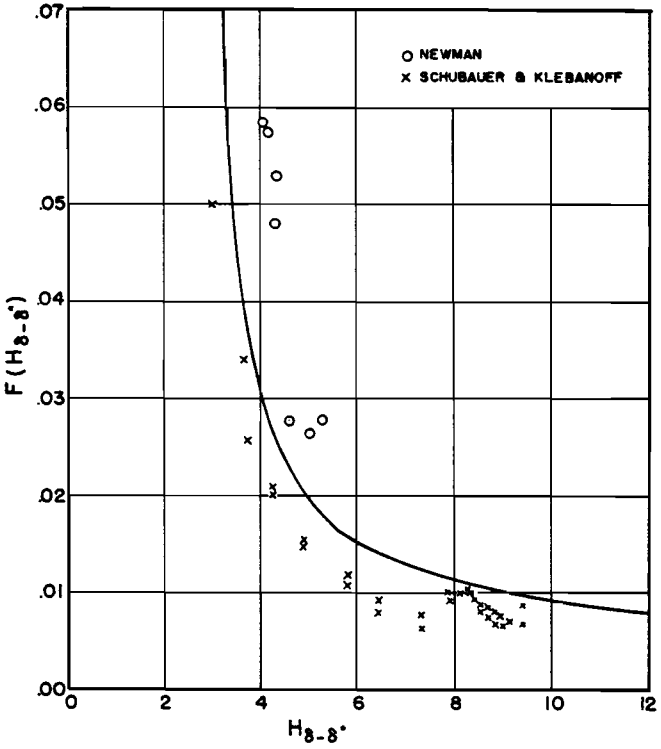

Fig.1. Correlation of Functions F and $H_{\Delta-\Delta^*}$, from Ref.(8)

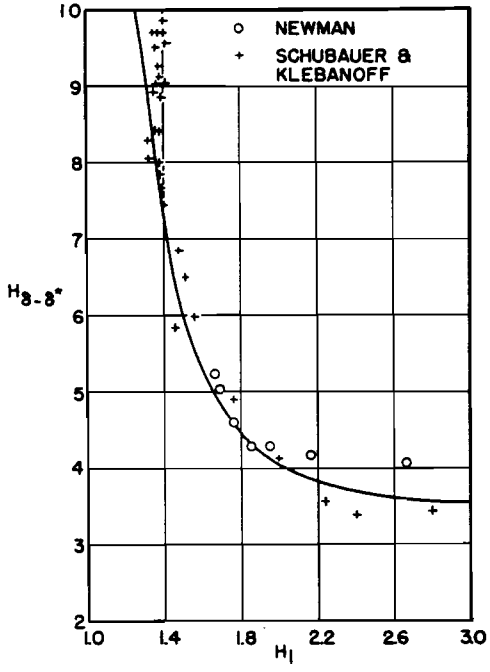

Fig.2. Correlation of Shape Factors $H_{\Delta-\Delta^*}$ and H_i, from Ref.(8)

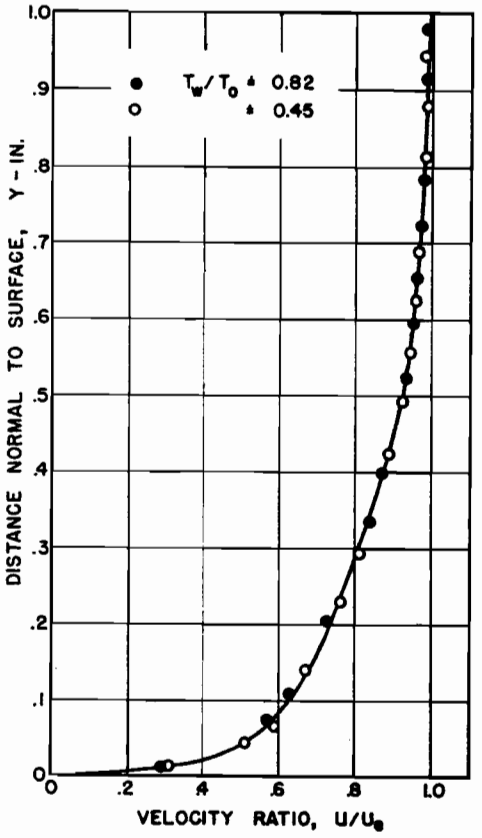

Fig.3. Velocity profiles at start of Compression, Isentropic surface, Ref.(6).

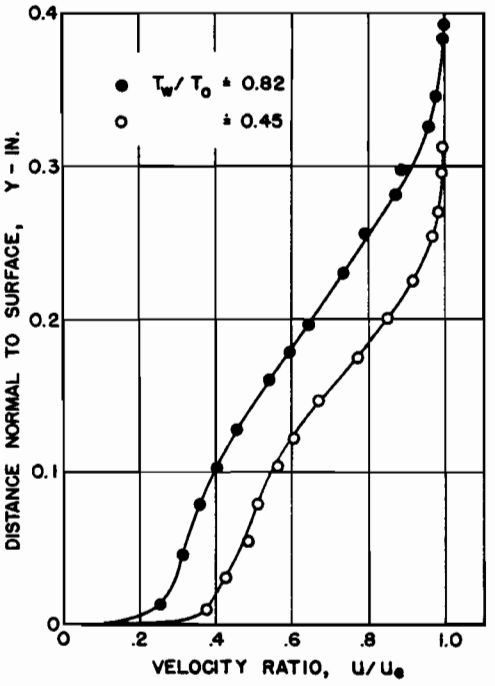

Fig.4. Velocity profiles in final stages of Compression, Isentropic surface, Ref.(6).

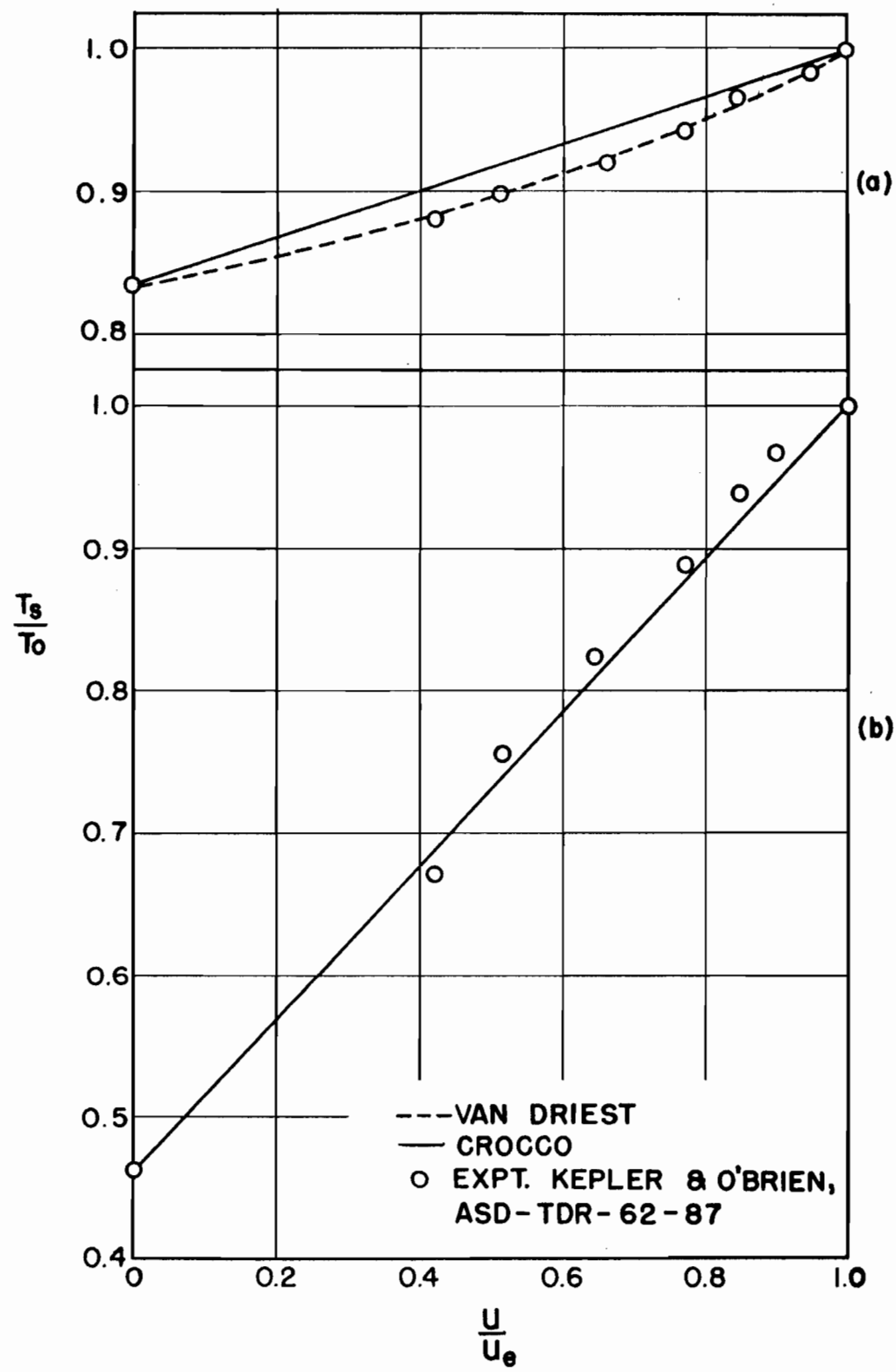

Fig.5. Temperature-velocity relations, Mach 3 flat plate and start of Compression on Circular Arc surface. (a) Tw/To ≐ .835 (b) Tw/to ≐ .460

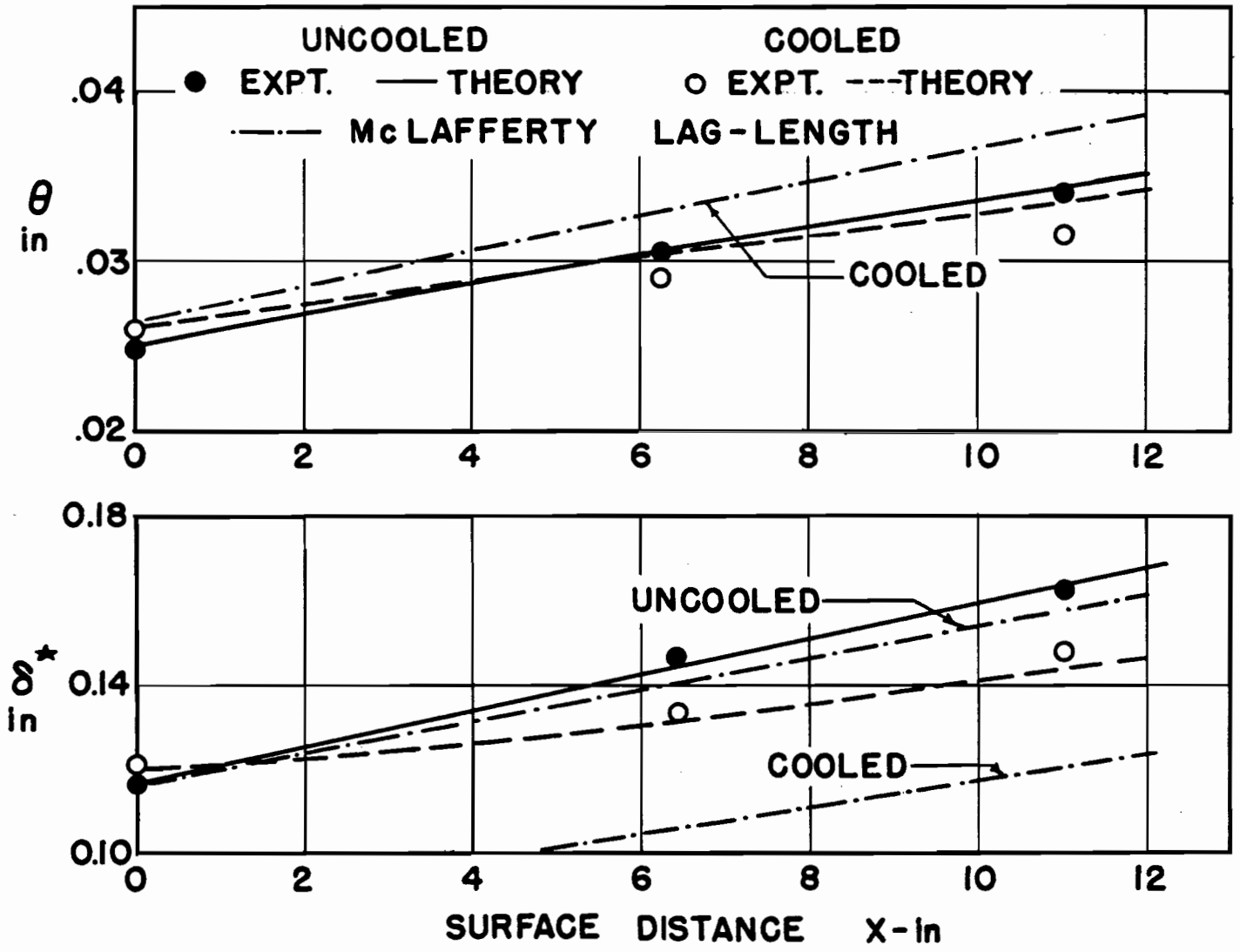

Fig.6. Variation of Momentum and Displacement Thicknesses on Mach 3 flat plate of Ref.(6). Uncooled Tw/To ≐ .835; Cooled Tw/To ≐ .460

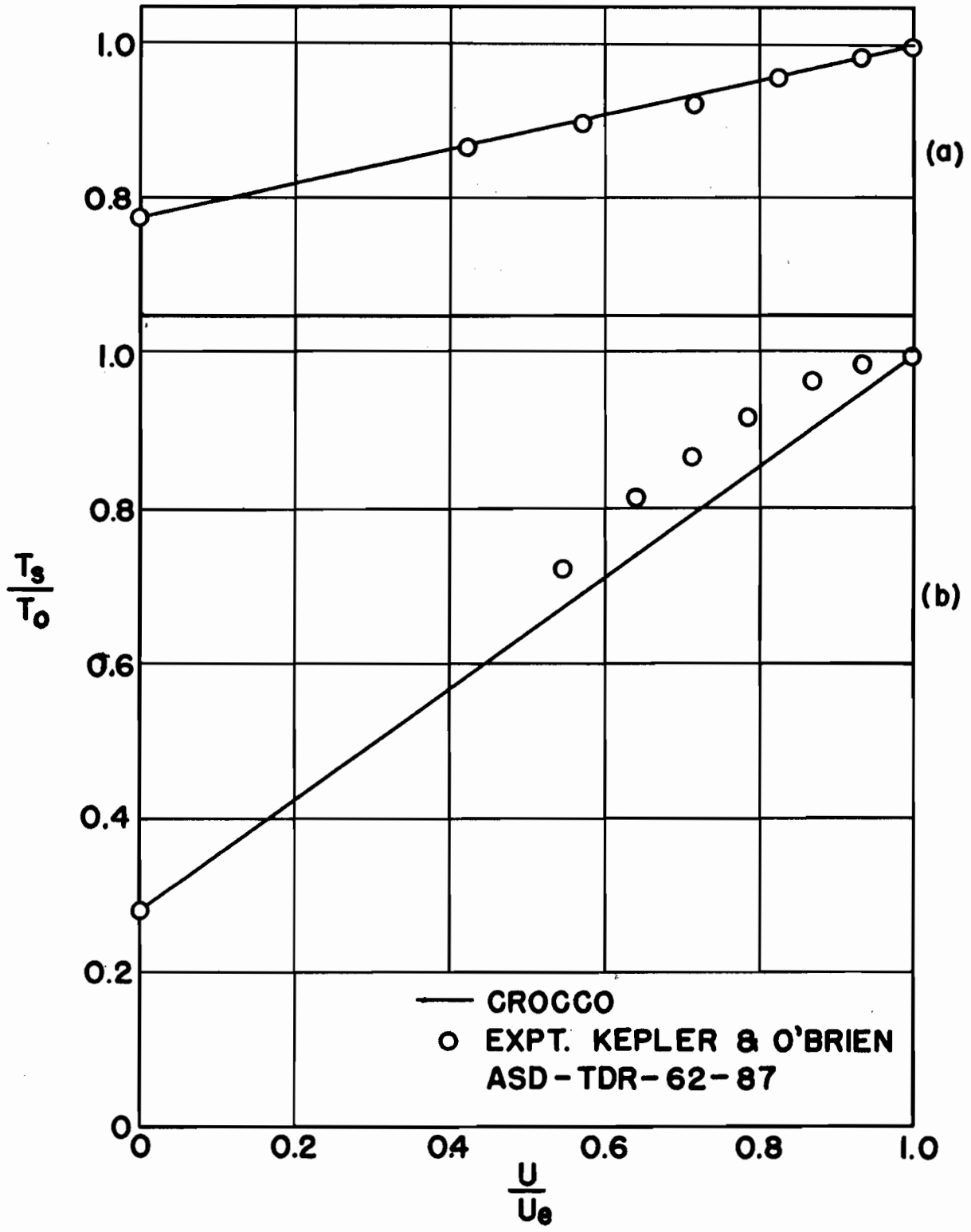

Fig.7. Temperature-velocity relations, Mach 6 flat plate of Ref.(6). Uncooled Tw/To ≐ .835; Cooled Tw/To ≐ .460

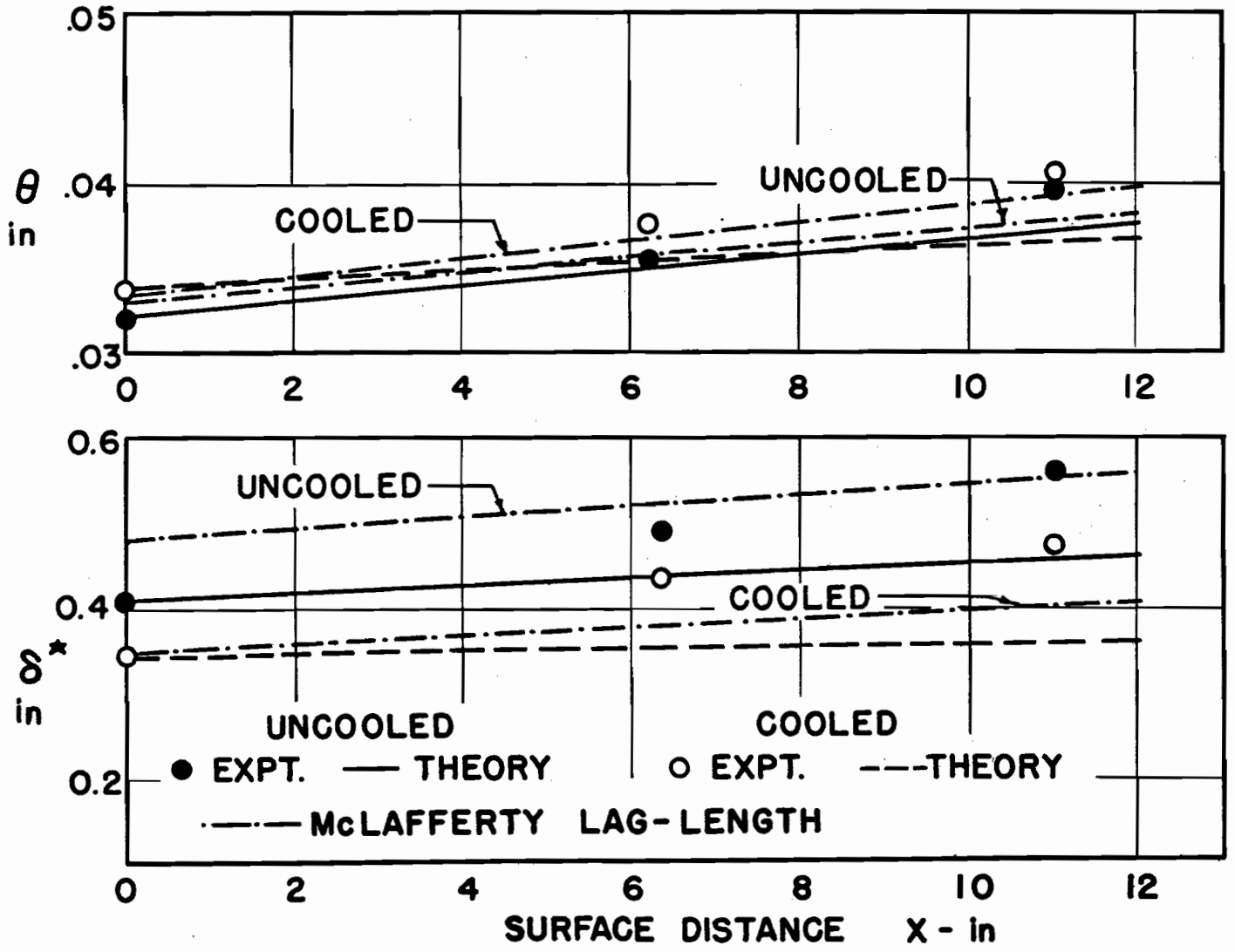

Fig.8. Variation of Momentum and Displacement Thicknesses on Mach 6 flat plate of Ref.(6). Uncooled Tw/To ≐ .76; Cooled Tw/To ≐ .28

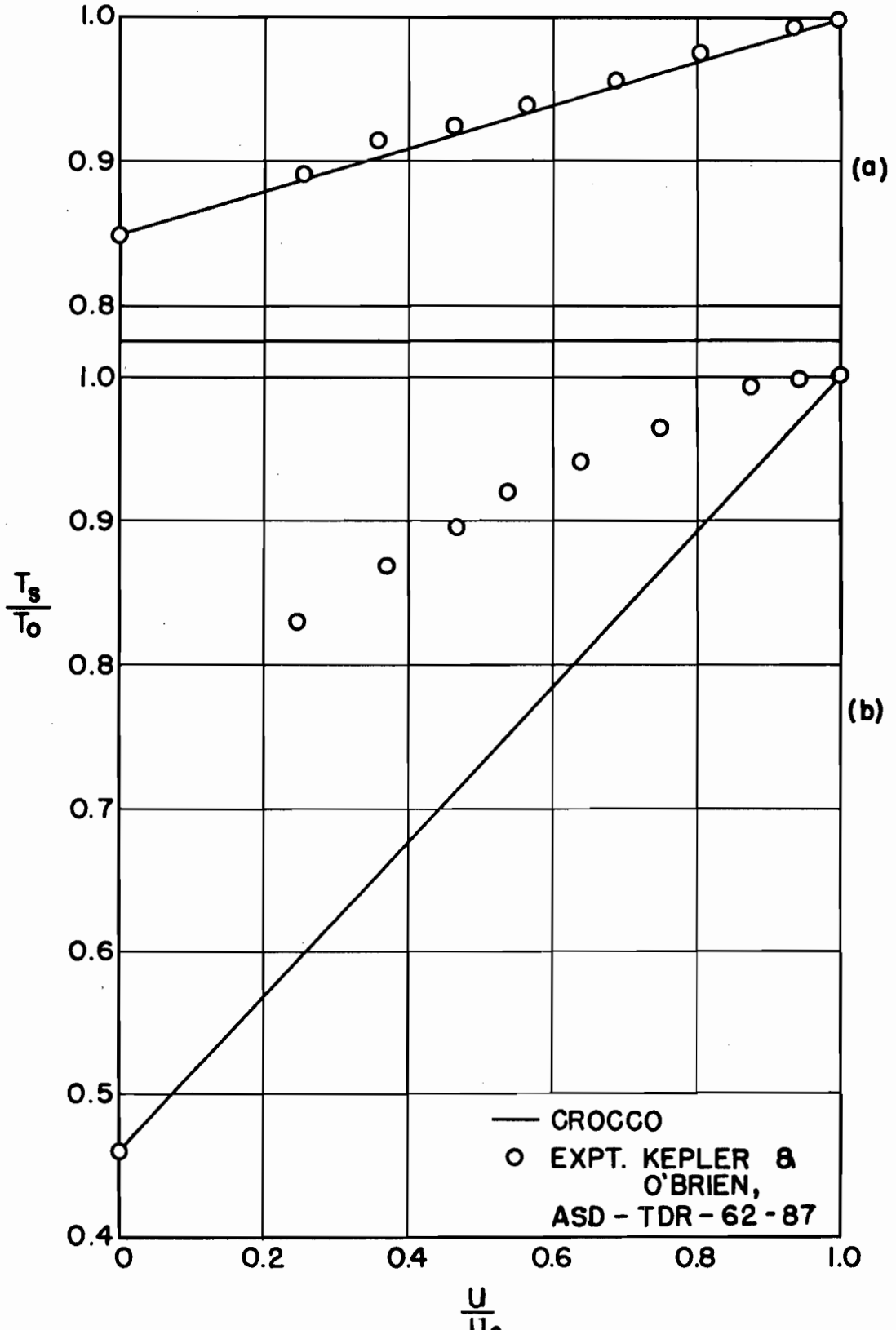

Fig.9. Temperature-velocity relations near end of compression, Mach 3 Circular Arc surface. (a) Tw/To ≐ .835 (b) Tw/To ≐ .460

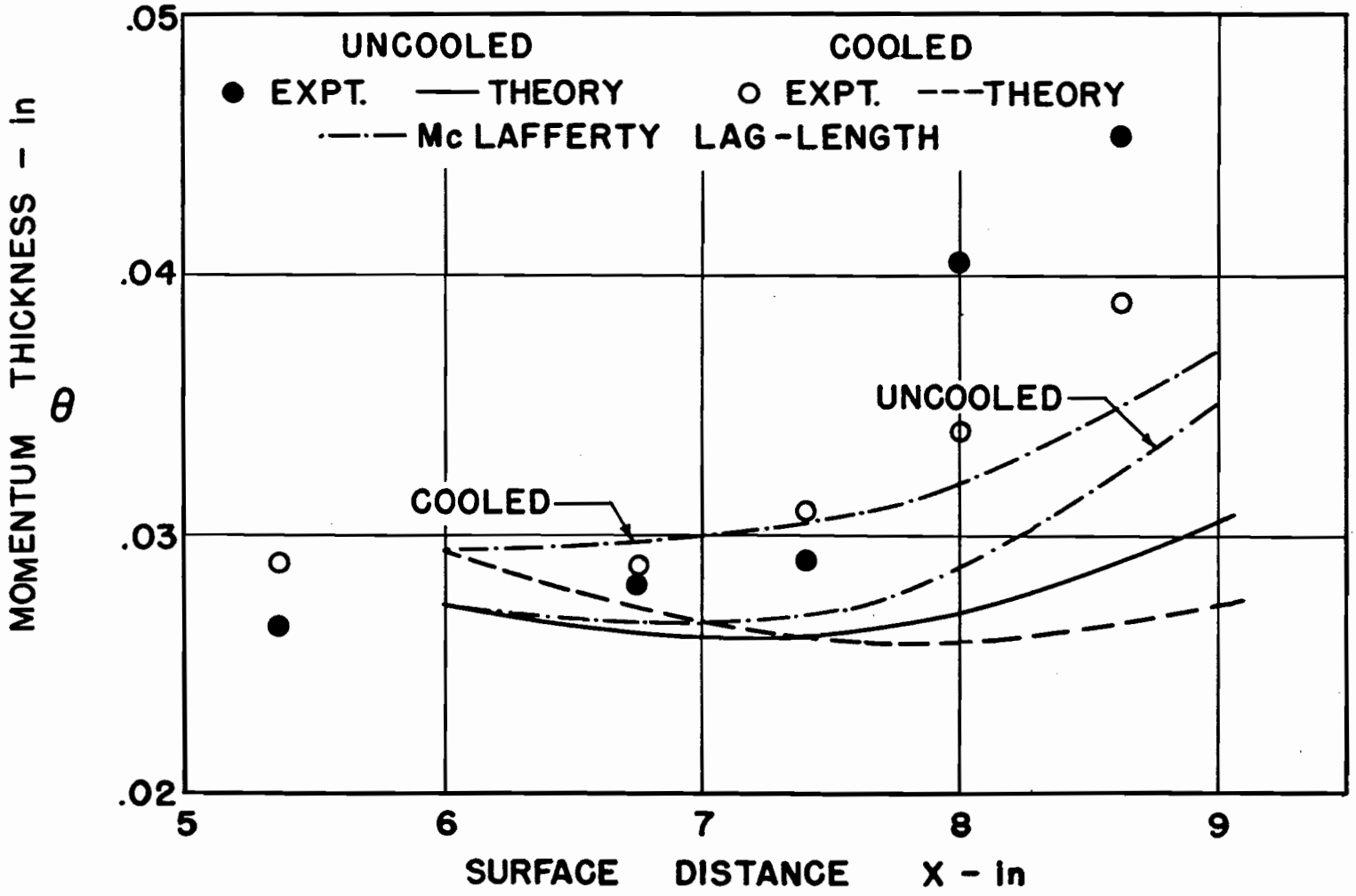

Fig.10. Variation of Momentum Thickness on Circular Arc surface of Ref.(6). Uncooled Tw/To ≐ .835; Cooled Tw/To ≐ .460

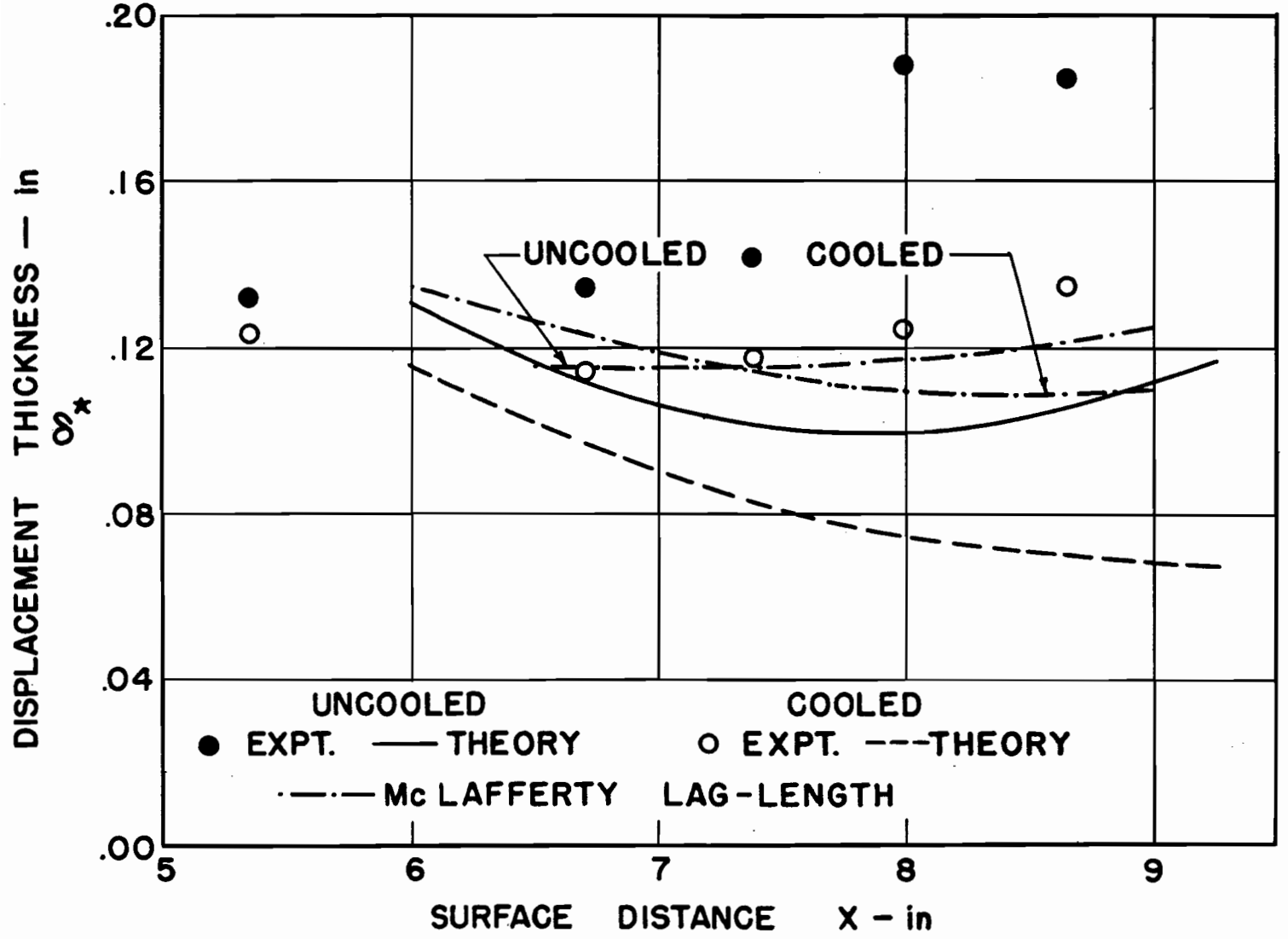

Fig.11. Variation of Displacement Thickness on Circular Arc surface of Ref.(6). Uncooled Tw/To ≐ .835; Cooled Tw/To ≐ .460

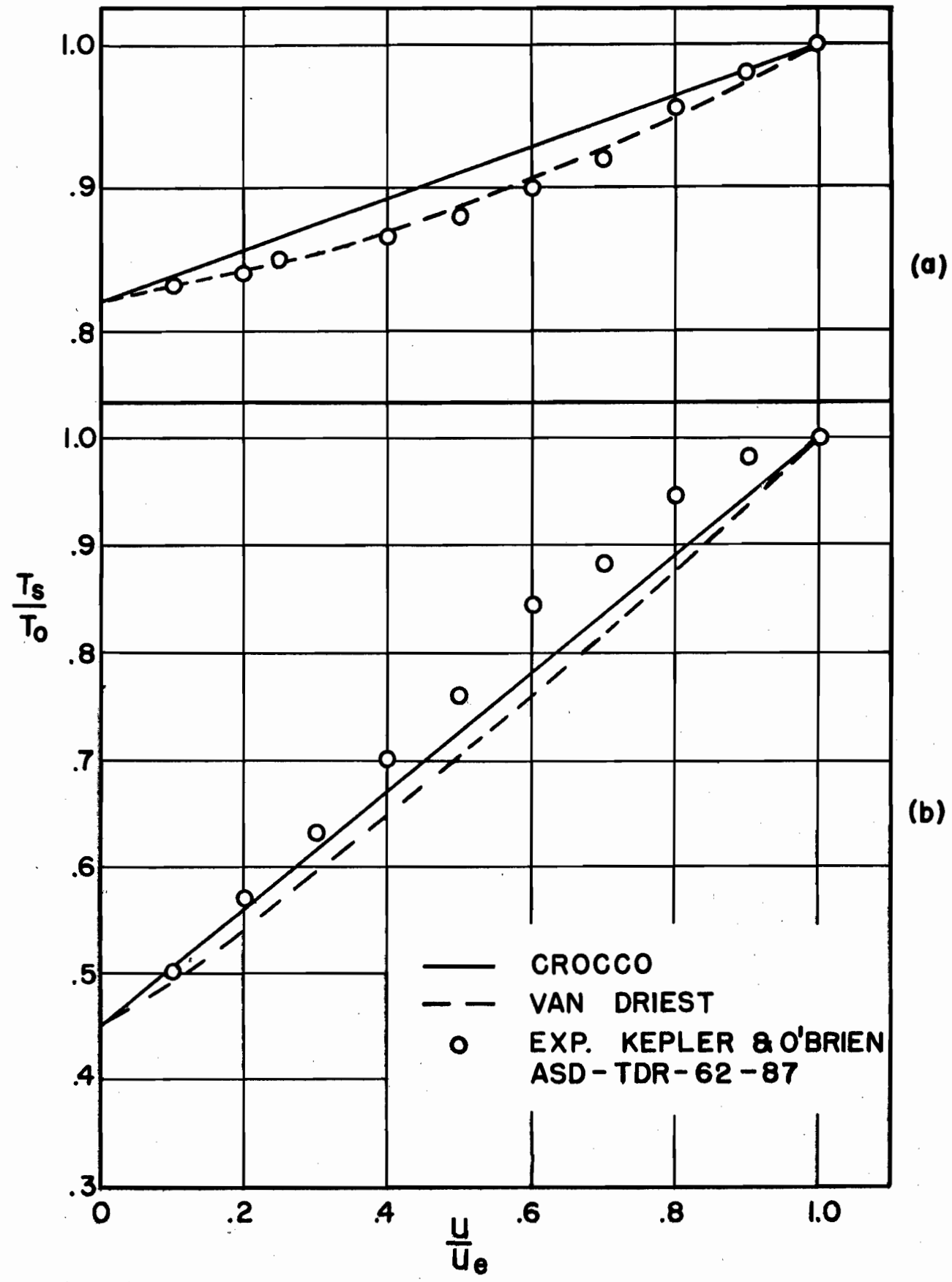

Fig.12. Temperature-velocity relations at start of compression, Isentropic surface of Ref.(6).
(a) Tw/To ≐ .82 (b) Tw/To ≐ .45

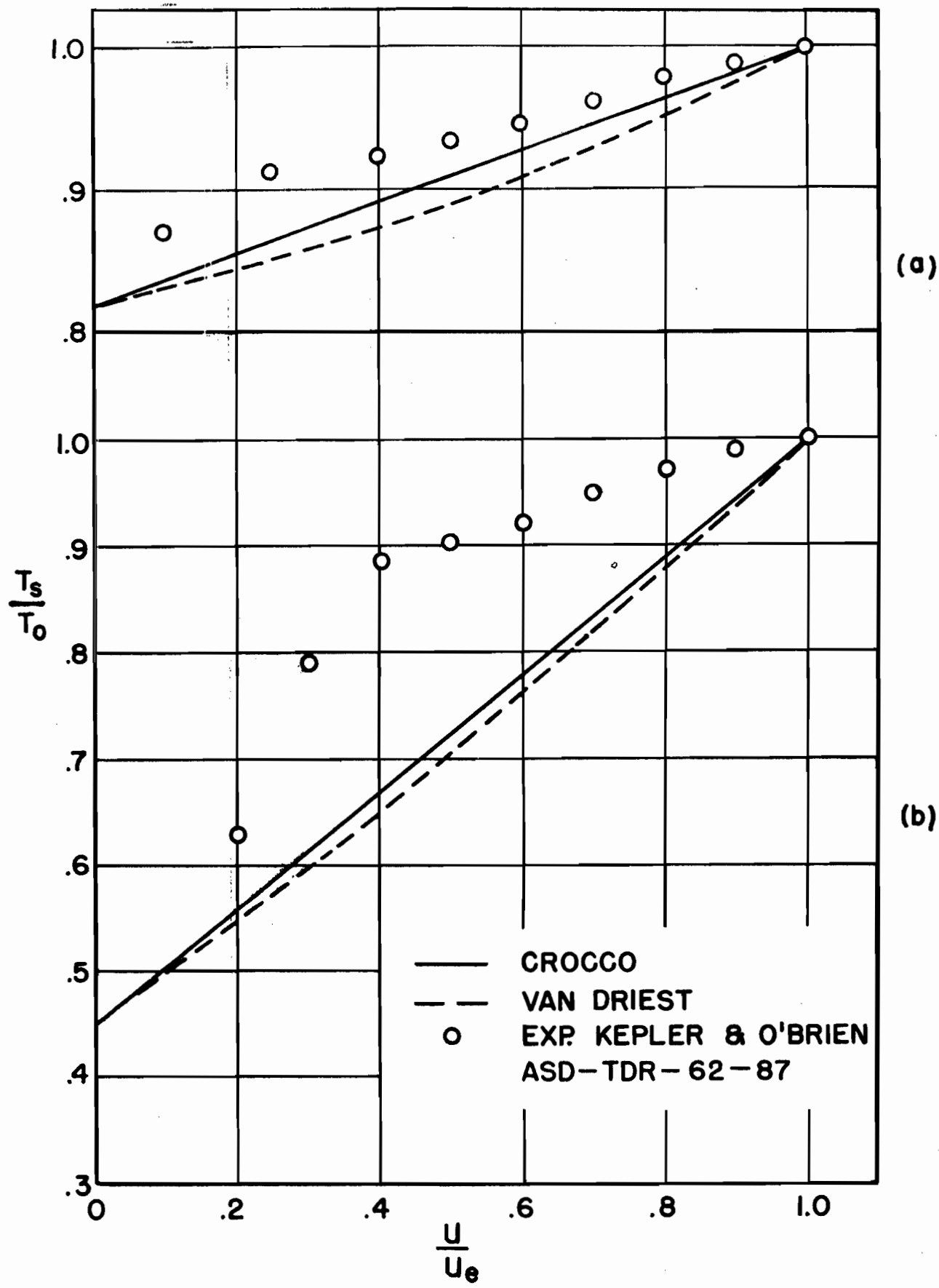

Fig.13. Temperature-velocity relations near end of compression, Isentropic surface of Ref.(6). (a) Tw/To ≐ .82 (b) Tw/To ≐ .45

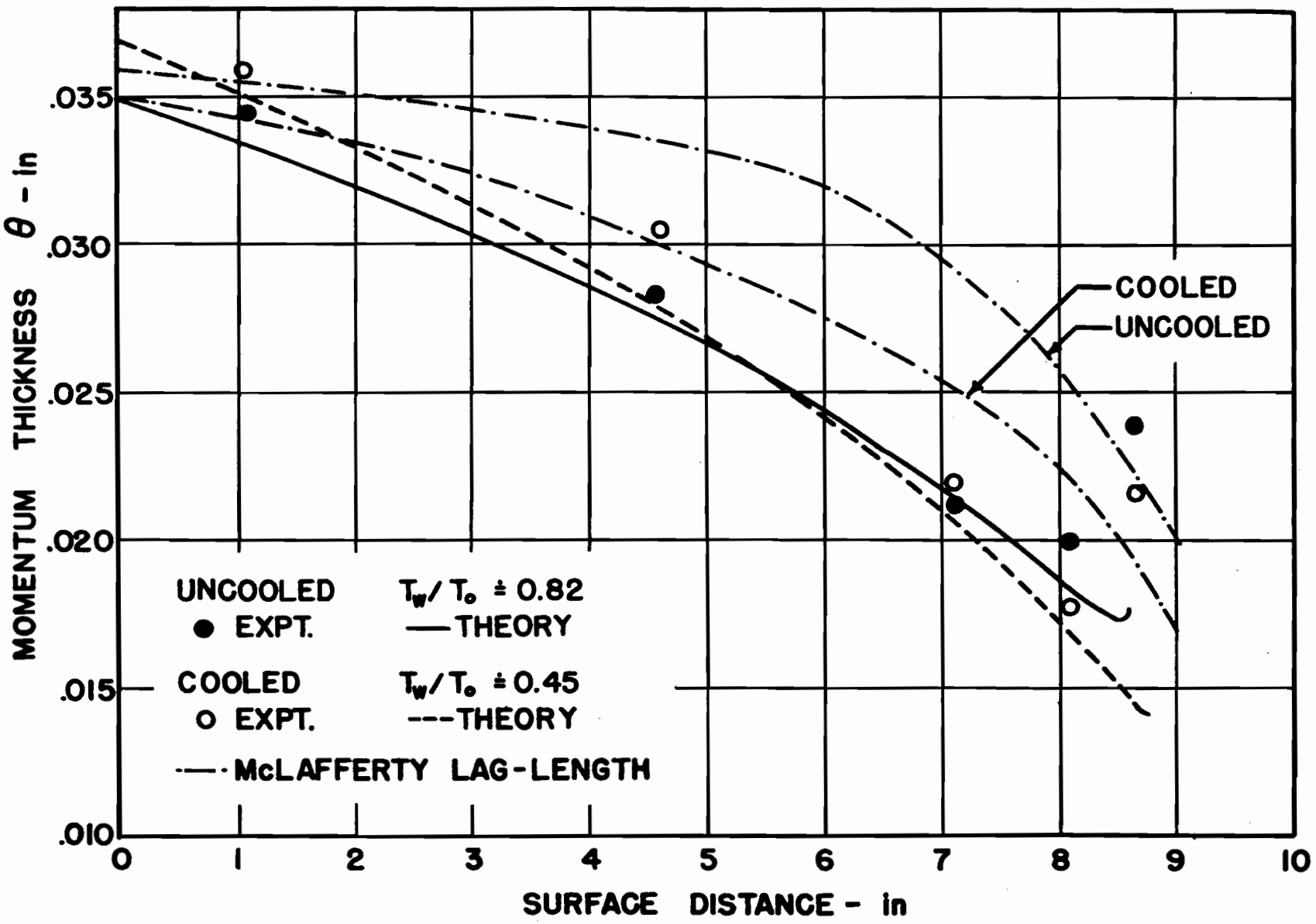

Fig.14. Variation of Momentum Thickness on Isentropic Compression Surface of Ref.(6)

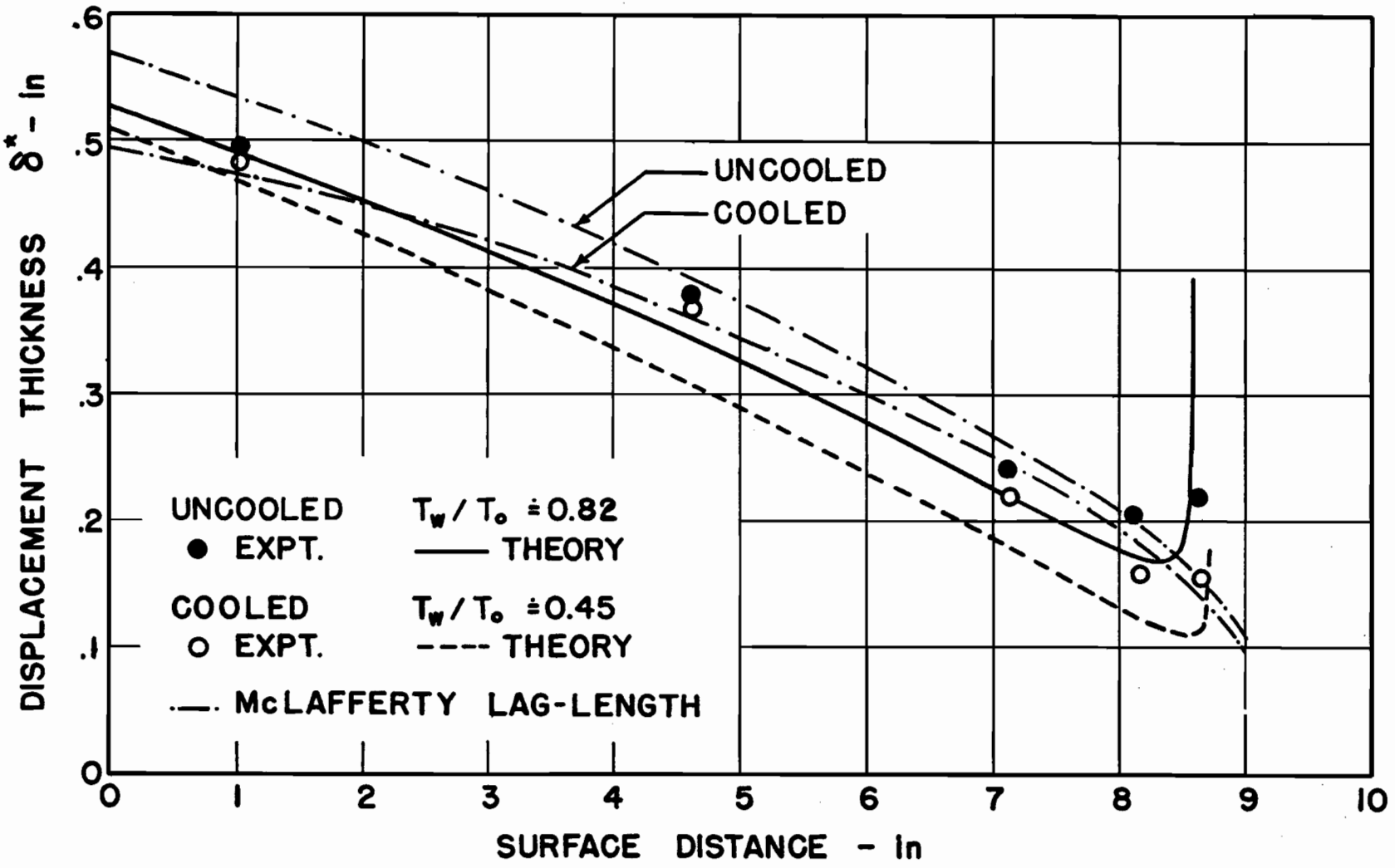

Fig.15. Variation of Displacement Thickness on Isentropic Compression Surface of Ref.(6)